Laser power calculations: sources of error

Lee W. Casperson

The physical phenomena that dominate the power characteristics of a laser depend on the detailed nature of the amplifying medium and the resonator structure. In predicting the power characteristics, numerous approximations are always required. The most important approximations are considered here in detail, and error estimates are presented so that a designer can select the appropriate model for a particular application. Emphasis is placed on analytic solutions and specific phenomena considered include longitudinal and transverse spatial hole burning, large single-pass gain, and mixed line broadening.

I. Introduction

One of the most important parameters of a laser oscillator is the total output power. For many applications one seeks to maximize the power output of a laser subject to constraints of size, efficiency, and cost. Unfortunately, this problem can become analytically difficult, and one never attempts an exact solution for even the simplest of laser configurations. The usual approach is to choose suitable approximations and obtain estimates of the maximum error that such choices will entail. Thus, it is helpful if simple realistic models are available for predicting the characteristics of particular laser designs.

The purpose of this paper is to bring together several basic laser models, which include most cw lasers of interest. Some of these models have been considered previously in one form or another, but, even for these cases, there has been little attention given to establishing the magnitude of the inevitable errors. Such error information is obviously necessary to ensure that a calculation is sufficiently accurate for a particular application. An equally important benefit of accurate error information is that one can avoid making unnecessarily precise corrections for one physical effect, while ignoring altogether other effects that might be more substantial. Time and cost spent on empirical optimization studies can also be reduced. A brief review of the simple power calculations usually encountered is presented in Sec. II. Each following section then treats a specific correction to the basic power formulas. These sections conclude with explicit analytic relationships between the one-way intensity in the laser cavity and the threshold parameter. These relationships are then plotted and compared with the simpler formulas of Sec. II. The internal intensity is chosen for display rather than the output intensity, because one less parameter (the mirror transmission) is involved.

Many modern lasers exhibit large values of the single-pass gain, and the usual perturbation calculations are inaccurate. Corrections for large single-pass gain are discussed in Sec. III. Section IV describes the corrections that result from recognizing that the fields in the laser oscillator are standing waves rather than traveling waves. These calculations are based on the familiar density matrix equations, and one finds that longitudinal spatial hole burning usually tends to reduce the laser intensity. If the atoms are in rapid motion this effect is eliminated, and the intensity may even be larger than otherwise expected. In Sec. V it is shown that transverse spatial hole burning tends to enhance the output intensity as even the wings of the electromagnetic field distribution are eventually able to saturate the amplifying medium. The effects of mixed line broadening are discussed in Sec. VI. It is always convenient to regard a laser as being either homogeneously or inhomogeneously broadened, but, in fact, all lasers are to some extent mixed cases.

II. Basic Concepts

To calculate the laser power for many single-mode applications, one takes as a starting point the relationship

$$\frac{dI}{dz} = g(\nu,I)I - \eta I, \tag{1}$$

where $g(\nu,I)$ is a gain coefficient depending on frequency

The author is with UCLA, School of Engineering & Applied Science, Los Angeles, California 90024.

Received 22 October 1979.
0003-6935/80/030422-13$00.50/0.

ν and intensity I, and η is a distributed loss coefficient. The solution to Eq. (1) can be obtained once an explicit form for $g(\nu,I)$ is assumed. The functional form of $g(\nu,I)$ depends on which broadening mechanisms are dominant in the particular laser medium being considered.

In a homogeneously broadened laser medium all the atoms (or molecules) are equivalent in the sense of having the same laser transition frequency, radiative lifetimes, and collision rates with other atoms or phonons. It can be shown that the stimulated emission coefficient for this type of medium has a Lorentzian frequency dependence.[1,2] Combining this result with a rate equation model for the atomic populations, one finds that the gain coefficient for a homogeneously broadened laser takes the form

$$g_h(\nu,I) = \frac{g_{ho}}{1 + [2(\nu - \nu_0)/\Delta\nu_h]^2 + sI}, \tag{2}$$

where g_{ho} is the line center unsaturated gain, $\Delta\nu_h$ is the full width at half-maximum of the unsaturated Lorentzian, ν_0 is the center frequency of the transition, and s is a saturation parameter.

In an inhomogeneously broadened laser medium, the atoms have different transition frequencies due to Doppler shifts, nonuniform Stark or Zeeman effects, or isotope shifts. In such a medium the net gain is obtained by summing up the gain functions like that in Eq. (2) for each frequency class of atoms. Thus, the inhomogeneous gain function can often be written

$$g_i(\nu,I) = g_{ho} \int_0^\infty \frac{p(\nu_a)d\nu_a}{1 + [2(\nu - \nu_a)/\Delta\nu_h]^2 + sI}, \tag{3}$$

where $p(\nu_a)$ is a normalized distribution of atomic center frequencies. If $p(\nu_a)$ is broad compared with $\Delta\nu_h$, the result of such a summation is

$$g_i(\nu,I) = g_{ho}p(\nu) \int_0^\infty \frac{d\nu_a}{1 + [2(\nu - \nu_a)/\Delta\nu_h]^2 + sI}$$

$$= \frac{g_{ho}p(\nu)(\pi\Delta\nu_h/2)}{(1 + sI)^{1/2}}. \tag{4}$$

In a Doppler broadened gas laser, for example, this line shape function is the Gaussian

$$p(\nu_a) = \frac{2(\ln 2)^{1/2}}{\pi^{1/2}\Delta\nu_D} \exp\left\{-\left[\frac{2(\nu_a - \nu_0)}{\Delta\nu_D}\right]^2 \ln 2\right\}, \tag{5}$$

where $\Delta\nu_D$ is the full Doppler width at half-maximum. Thus the inhomogeneous gain of Eq. (4) is

$$g_i(\nu,I) = \frac{g_{io} \exp\{-[2(\nu - \nu_0)/\Delta\nu_D]^2 \ln 2\}}{(1 + sI)^{1/2}}, \tag{6}$$

where the line center unsaturated gain g_{io} is relatated to g_{ho} by

$$g_{io} = g_{ho} \frac{\Delta\nu_h}{\Delta\nu_D} (\pi \ln 2)^{1/2}. \tag{7}$$

Using the homogeneous or inhomogeneous gain distributions given, respectively, in Eqs. (2) and (6), one can apply Eq. (1) to a variety of laser problems. Thus, the intensity in a homogeneously broadened laser amplifier is governed by the equation

$$\frac{dI}{dz} = \frac{g_{ho}I}{1 + [2(\nu - \nu_0)/\Delta\nu_h]^2 + sI} - \eta I. \tag{8}$$

In a low-gain laser oscillator the intensity of the waves traveling to the right and to the left are approximately equal, and one can replace the term sI by $2sI$ to reflect the fact that the gain is saturated by both waves. It then follows that the increase in intensity after one round trip in a low-gain laser oscillator can be written

$$\Delta I = \frac{2g_{ho}lI}{1 + [2(\nu - \nu_0)/\Delta\nu_h]^2 + 2sI} - 2\eta lI, \tag{9}$$

where l is the length of the amplifying medium. On the other hand, the mirror loss after one round trip is

$$\Delta I = (1 - R_l)I + (1 - R_r)I, \tag{10}$$

where R_l and R_r are, respectively, the reflectivities of the left-hand and right-hand mirrors.

For stable oscillation the round-trip gain must equal the round-trip loss so the left-hand sides of Eqs. (9) and (10) are equal. The resulting equation may be solved for the intensity I, and one obtains

$$I = \frac{1}{2s}\left\{\frac{2g_{ho}l}{(1 - R_l) + (1 - R_r) + 2\eta l} - 1 - \left[\frac{2(\nu - \nu_0)}{\Delta\nu_h}\right]^2\right\}. \tag{11}$$

The output intensity at the right or left end of the laser is obtained by multiplying the intensity of Eq. (11) by the appropriate mirror transmission. The frequency term vanishes if the laser is tuned to line center, or it may be absorbed into the gain and saturation parameters. Then Eq. (11) can be written simply

$$sI = (r - 1)/2, \tag{12}$$

where r is a threshold coefficient representing the ratio of round-trip gain to loss. In one form or another this is the familiar and widely employed expression for the intensity in a homogeneously broadened laser oscillator. From it may be derived the output intensity and optimum coupling conditions. One purpose of the following sections is to investigate in detail the numerous sources of error that may severely limit the accuracy of these results.

A similar analysis applies to inhomogeneously broadened lasers. From Eqs. (1) and (6) the intensity in a laser amplifier must satisfy

$$\frac{dI}{dz} = \frac{g_{io} \exp\{-[2(\nu - \nu_0)/\Delta\nu_D]^2 \ln 2\}}{(1 + sI)^{1/2}} - \eta I. \tag{13}$$

The frequency dependence can again be incorporated into the gain coefficient. The same analysis as employed for the homogeneous case yields the result

$$sI = (r^2 - 1)/2. \tag{14}$$

In this case the gain is a quadratic function of r rather than being a linear function.

Equation (14) applies directly for most types of inhomogeneous broadening. However, in a Doppler broadened medium tuned away from line center the right and left traveling waves interact with different velocity classes of atoms, and the factor of 2 should be

deleted from Eq. (14). This relative decrease in intensity near line center is the familiar Lamb dip, which is typical of many gas lasers.[3]

III. Large Single-Pass Gain

A. Homogeneously Broadened Lasers

The emphasis in Sec. II was on lasers in which the gain per pass is small compared to unity. It is now appropriate to consider in detail the limitations on the validity of the low-gain approximation. In a homogeneously broadened laser, the equations governing the intensity of the wave traveling to the right I^+ and the intensity of the wave traveling to the left I^- can be written[4,5]

$$\frac{dI^+}{dz} = \frac{g_{ho}I^+}{1 + s(I^+ + I^-)} - \eta I^+, \tag{15}$$

$$\frac{dI^-}{dz} = \frac{-g_{ho}I^-}{1 + s(I^+ + I^-)} + \eta I^-. \tag{16}$$

For simplicity it has been assumed that the laser is operating at line center. This assumption does not actually reduce the generality of the analysis, since off-center frequencies can be represented by including a Lorentzian frequency factor in the gain and saturation parameters. Also it may be noted here that saturation depends on the sum of the electric fields rather than on the intensities, and the resultant longitudinal spatial hole burning is discussed in Sec. IV. However, in high-gain lasers the effective standing wave region is short, and spatial hole burning (which will be found to be small anyway) can have little effect on the output.

It follows readily from Eqs. (15) and (16) that the product of the intensities of the waves traveling to the left and to the right is a constant independent of z, i.e.,

$$I^+(z)I^-(z) = \text{const.} \tag{17}$$

With a bit more algebra one can find, for example, that the intensity incident on the right-hand mirror in a high-gain laser with negligible distributed losses is

$$2sI^+(z_r) = [(1 - R_r) + (R_r/R_l)^{1/2}(1 - R_l)]^{-1}[2g_{ho}l + \ln(R_lR_r)]. \tag{18}$$

In an optimized system the reflectivity of the left-hand mirror would, it is hoped, be close to unity, and thus Eq. (18) reduces to

$$2sI^+(z_r) = (1 - R_r)^{-1}(2g_{ho}l + \ln R_r). \tag{19}$$

The threshold parameter is related to the gain and loss by

$$r = -2g_{ho}l/\ln R_r. \tag{20}$$

Therefore, Eq. (19) can also be written

$$sI^+(z_r) = \frac{g_{ho}l(1 - r^{-1})}{1 - \exp(-2g_{ho}l/r)}. \tag{21}$$

Equation (21) is plotted in Fig. 1 for various values of the unsaturated single-pass gain $g_{ho}l$. From this figure it is apparent that, at moderate levels of gain, the laser intensity may be many times larger than the values predicted by the standard low-gain formula $(r - 1)/2$ given in Eq. (12).

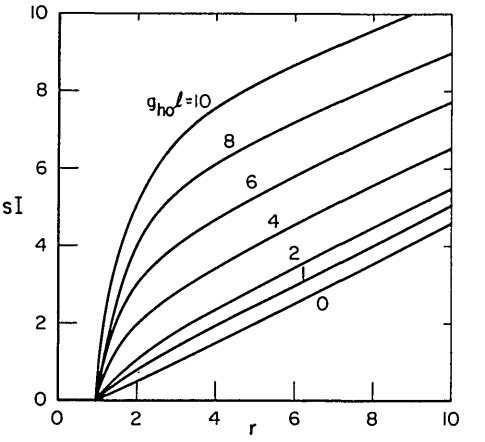

Fig. 1. Normalized intensity sI incident on the coupling mirror of a high-gain homogeneously broadened laser as a function of the threshold parameter r for various values of the single-pass gain. The curve labeled $g_{ho}l = 0$ is the same as the standard low-gain approximation of Eq. (12).

B. Non-Doppler Inhomogeneously Broadened Lasers

As shown previously in Sec. II, the saturation formulas for homogeneous and inhomogeneous saturation are similar except that here a square root is needed in the saturation terms. Thus, Eqs. (15) and (16) must now be replaced by the set

$$\frac{dI^+}{dz} = \frac{g_iI^+}{[1 + s(I^+ + I^-)]^{1/2}} - \eta I^+, \tag{22}$$

$$\frac{dI^-}{dz} = \frac{-g_iI^-}{[1 + s(I^+ + I^-)]^{1/2}} + \eta I^-. \tag{23}$$

The inhomogeneous gain coefficient is assumed to include the frequency dependence of the transition.

Equations (22) and (23) cannot be solved without making some fairly restrictive approximations. Numerical solutions are straightforward, however, and some typical results are given in Fig. 2 for the cases $R_l = 0$ and $\eta = 0$. As in the homogeneous case, the discrepancy between the actual intensity and the low-gain approximation $(r^2 - 1)/2$ of Eq. (14) may be very substantial.

C. Doppler Inhomogeneous Broadening

As we have seen in Sec. II, with Doppler broadening the right and left traveling waves may or may not both interact with the same atoms depending on the frequency tuning of the mode with respect to line center. The general behavior is difficult to represent, so we consider here only the two important limits. For frequencies close to line center, both waves interact with the same atoms, and the saturation equations are identical with Eqs. (22) and (23). Hence, this limit does

not need to be discussed further. For frequencies far from line center compared to the homogeneous linewidth $\Delta\nu_h$, the waves interact with different classes of atoms, and the saturation equations are

$$\frac{dI^+}{dz} = \frac{g_i I^+}{(1+sI^+)^{1/2}} - \eta I^+, \tag{24}$$

$$\frac{dI^-}{dz} = \frac{-g_i I^-}{(1+sI^-)^{1/2}} + \eta I^-, \tag{25}$$

where g_i is the unsaturated gain at the laser frequency. These equations form the basis of the following discussion.

The first feature of Eqs. (24) and (25) to be noted is that they are entirely decoupled. If the reflectivity of the left-hand mirror is unity, one can simply integrate a single equation for two passes through the amplifier, and the result is[6]

$$2g_i l = \ln\left[\frac{(1+sI_2)^{1/2}-1}{(1+sI_2)^{1/2}+1} \times \frac{(1+sI_1)^{1/2}+1}{(1+sI_1)^{1/2}-1}\right] + 2(1+sI_2)^{1/2} - 2(1+sI_1)^{1/2}, \tag{26}$$

where I_1 is the intensity before the round trip, I_2 is the intensity afterward, and distributed losses have again been neglected ($\eta = 0$). The boundary condition at the transmitting mirror is $I_1 = RI_2$, so Eq. (26) can be written

$$2g_i l = \ln\left[\frac{(1+sI_2)^{1/2}-1}{(1+sI_2)^{1/2}+1} \times \frac{(1+RsI_2)^{1/2}+1}{(1+RsI_2)^{1/2}-1}\right] + 2(1+sI_2)^{1/2} - 2(1+RsI_2)^{1/2}. \tag{27}$$

This is a single equation in the unknown function I_2, and solutions can be readily obtained by iteration. The results can also be expressed in terms of the gain $g_i l$ instead of the mirror reflectivity R by means of the inhomogeneous analog of Eq. (20).

Equation (27) is plotted in Fig. 3 for various values of the gain $g_i l$. Again it may be seen that, for moderate values of gain, the intensity is much larger than the low-gain limit $r^2 - 1$.

IV. Longitudinal Spatial Burning

A. Homogeneous Broadening

A second potential source of error in laser power calculations concerns longitudinal spatial hole burning.[7] Due to this effect, the standing wave character of the resonator mode causes the gain saturation to be a strong function of longitudinal position. Some aspects of this effect can be understood in terms of rate equation models, but a complete discussion must be based on a more general semiclassical approach. A brief density matrix derivation of the basic equations is given in the Appendix, and we consider here the results of those calcuations.

For a laser medium having negligible Doppler broadening, the semiclassical analysis yields two coupled equations for the mode intensity and frequency:

$$\frac{1}{2t_c} = \frac{\omega_0 \mu^2}{\epsilon_0 L \gamma \hbar} \int_0^\infty \int_0^l \frac{\sin^2(kz) N(\omega_a) dz d\omega_a}{1 + [(\omega - \omega_a)/\gamma]^2 + 4\sin^2(kz) sI}, \tag{28}$$

$$\omega - \Omega = \frac{\omega_0 \mu^2}{\epsilon_0 L \gamma \hbar} \int_0^\infty \int_0^l \left(\frac{\omega_a - \omega}{\gamma}\right) \times \frac{\sin^2(kz) N(\omega_a) dz d\omega_a}{1 + [(\omega - \omega_a)/\gamma]^2 + 4\sin^2(kz) sI}, \tag{29}$$

where t_c is the cavity lifetime, μ is the transition matrix element, l is the length of the amplifying medium, L is the length of the cavity, γ is the phase relaxation rate, and $N(\omega_a)$ is the unsaturated population inversion as a function of the atomic frequencies ω_a. The electric field is assumed to have a $\sin(kz)$ longitudinal dependence, and these equations given also as (A27) and (A28) apply for both homogeneous and non-Doppler inhomogeneous broadening.

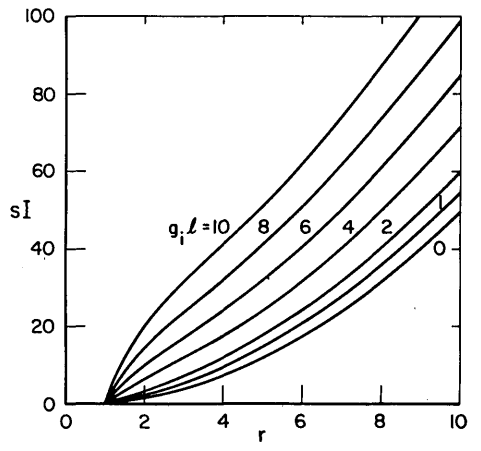

Fig. 2. Normalized intensity sI incident on the coupling mirror of a high-gain non-Doppler inhomogeneously broadened laser for various values of the single-pass gain. The curve labeled $g_i l = 0$ is the same as the standard low-gain approximation of Eq. (14).

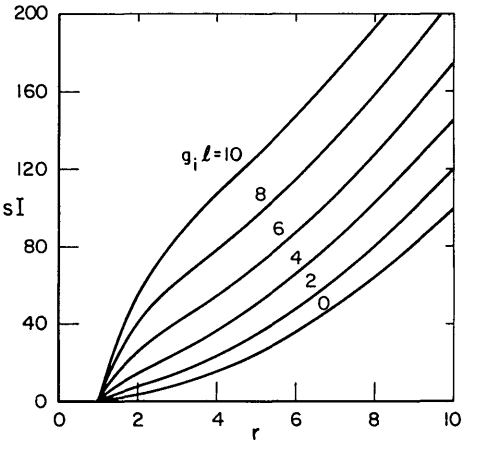

Fig. 3. Normalized intensity sI incident on the coupling mirror of a high-gain Doppler laser tuned away from line center for various values of the single-pass gain. The curve labeled $g_i l = 0$ is the same as the standard low-gain approximation $r^2 - 1$.

In the homogeneous limit the function $N(\omega_a)$ is very narrow compared to the Lorentzian terms and is centered at the frequency ω_0. Thus Eqs. (28) and (29) can be written

$$\frac{1}{2t_c} = \frac{\omega_0 \mu^2 N}{\epsilon_0 L \gamma \hbar} \int_0^l \frac{\sin^2(kz)dz}{1 + [(\omega - \omega_0)/\gamma]^2 + 4\sin^2(kz)sI}, \tag{30}$$

$$\omega - \Omega = \frac{\omega_0 \mu^2 N}{\epsilon_0 L \gamma \hbar} \left(\frac{\omega_0 - \omega}{\gamma}\right) \int_0^l \frac{\sin^2(kz)dz}{1 + [(\omega - \omega_0)/\gamma]^2 + 4\sin^2(kz)sI}, \tag{31}$$

where

$$N = \int_0^\infty N(\omega_a)d\omega_a$$

is the total population difference. With some simple manipulations these integrals may be put into a standard form, and the results are[8]

$$1 = 2r\left(1 + \frac{4sI}{1 + [\omega - \omega_0)/\gamma]^2} + \left\{1 + \frac{4sI}{1 + [(\omega - \omega_0)/\gamma]^2}\right\}^{1/2}\right)^{-1}, \tag{32}$$

$$(\omega - \Omega)t_c = r\left(\frac{\omega_0 - \omega}{\gamma}\right)\left(1 + \frac{4sI}{1 + [(\omega - \omega_0)/\gamma]^2} + \left\{1 + \frac{4sI}{1 + [(\omega - \omega_0)/\gamma]^2}\right\}^{1/2}\right)^{-1}, \tag{33}$$

where r is a threshold parameter given by

$$r = \frac{t_c \omega_0 \mu^2 N l}{\epsilon_0 \gamma \hbar L}\left[1 + \left(\frac{\omega - \omega_0}{\gamma}\right)^2\right]^{-1}. \tag{34}$$

For values of r greater than unity the laser is above threshold and produces a nonzero output.

Equations (32) and (33) can be readily solved for the intensity and frequency of the laser mode. Thus Eq. (32) is basically a quadratic equation, and the solution is

$$\frac{sI}{1 + [(\omega - \omega_0)/\gamma]^2} = \frac{4r - 1 - (8r + 1)^{1/2}}{8}. \tag{35}$$

In practice the actual oscillation frequency ω is usually almost identical to the empty cavity frequency Ω, and the difference $\omega - \Omega$ is unimportant. Here, however, the frequency can be obtained exactly. Substituting Eq. (32) into Eq. (33) yields

$$(\omega - \Omega)t_c = \frac{\omega_0 - \omega}{2\gamma}. \tag{36}$$

Since the product $2\gamma t_c$ is usually large compared to unity, this result implies a slight mode pulling toward gain center. The explicit solution is

$$\omega = (\Omega + \omega_0/2\gamma t_c)(1 + 1/2\gamma t_c)^{-1}, \tag{37}$$

which may be used to eliminate ω from r in Eq. (34) and from Eq. (35). If the laser is tuned to line center ($\omega = \Omega = \omega_0$), Eq. (35) is simply

$$sI = \frac{4r - 1 - (8r + 1)^{1/2}}{8}. \tag{38}$$

Equations (12) and (38) are plotted for comparison in Fig. 4. It is evident from this comparison that, for any given value of the threshold parameter r, spatial hole burning has the effect of reducing the intensity by about 20 or 30%. It is reasonable that such a reduction should occur, since the standing wave fields cannot interact effectively with atoms that are situated near the field nodes. The largest discrepancy occurs near threshold ($sI \ll 1$), where Eq. (38) reduces to

$$sI \simeq (r - 1)/3. \tag{39}$$

Comparing Eqs. (12) and (39) one finds that ignoring spatial hole burning leads to a 50% overestimate of the laser intensity. It is important to note that Eq. (38) is not significantly more difficult to apply than is the much less accurate formula found previously.

B. Non-Doppler Inhomogeneous Broadening

In the solution of Eqs. (28) and (29) it was previously assumed that the function $N(\omega_a)$ was very narrow compared to the Lorentzian factors. This assumption led to the homogeneous saturation limit. However, for many lasers the opposite limit of inhomogeneous broadening is more appropriate. In this case the function $N(\omega_a)$ is broad compared to the Lorentzian and to first order it may be removed from the integrals leaving

$$\frac{1}{2t_c} = \frac{\omega_0 \mu^2 N(\omega)}{\epsilon_0 L \gamma \hbar} \int_0^l \int_0^\infty \frac{\sin^2(kz)d\omega_a dz}{1 + [(\omega - \omega_a)/\gamma]^2 + 4\sin^2(kz)sI}, \tag{40}$$

$$\omega - \Omega = \frac{\omega_0 \mu^2 N(\omega)}{\epsilon_0 L \gamma \hbar} \int_0^l \int_0^\infty \left(\frac{\omega_a - \omega}{\gamma}\right) \times \frac{\sin^2(kz)d\omega_a dz}{1 + [(\omega - \omega_a)/\gamma]^2 + 4\sin^2(kz)sI}. \tag{41}$$

An accurate calculation of the oscillation frequency would require some knowledge of the function $N(\omega_a)$. For the present purposes mode pulling is neglected by transforming the frequency integration in Eq. (41) to an integration over the difference $\omega_a - \omega$ and extending the lower limit from $-\omega$ to $-\infty$. In this approximation the integral vanishes since the integrand is an odd function of $\omega_a - \omega$. The frequency integration in Eq. (40) can be readily performed, and the result is

$$\frac{1}{2t_c} = \frac{\pi \omega_0 \mu^2 N(\omega)}{\epsilon_0 L \hbar} \int_0^l \frac{\sin^2(kz)dz}{[1 + 4sI\sin^2(kz)]^{1/2}}. \tag{42}$$

Since the range of integration is much greater than a wavelength, we may first average the integrand using the integral[9]

$$\int_0^{\pi/2} \frac{\sin^{2\mu-1}x \cos^{2\nu-1}x dx}{(1 - a^2\sin^2 x)^\rho} = \frac{B(\mu,\nu)F(\rho,\mu;\mu + \nu;a^2)}{2}, \tag{43}$$

where B is a β function, and F is a hypergeometric function. The final result is

$$\frac{1}{2t_c} = \frac{\omega_0 \mu^2 N(\omega) l}{\epsilon_0 \hbar L} B(3/2,1/2)F(1/2,3/2;2;-4sI). \tag{44}$$

The value of this β function is $\pi/2$, so Eq. (44) can be

written simply[10]

$$1 = rF(\tfrac{1}{2},\tfrac{3}{2};2;-4sI), \tag{45}$$

where the threshold parameter is defined by

$$r = \frac{\pi\omega_0 t_c \mu^2 N(\omega) l}{\epsilon_0 \hbar L}. \tag{46}$$

Equations (14) and (45) are plotted for comparison in Fig. 4. As in the case of homogeneous broadening, spatial hole burning has the effect of reducing the intensity. The largest percent discrepancy occurs near threshold where the hypergeometric function has the first-order approximation[11]

$$\frac{1}{r} = 1 - \tfrac{3}{2}sI + \ldots. \tag{47}$$

This result suggests the alternative approximation

$$r \simeq (1 + 3sI)^{1/2}. \tag{48}$$

From these results it is clear that again the neglect of spatial hole burning leads to a substantial overestimate of the laser intensity, and near threshold this overestimate amounts to 50%. It should also be noted that, for laser operation with r reasonably close to threshold, Eq. (48) provides a useful replacement for the somewhat cumbersome hypergeometric function. Equation (48) may be inverted explicitly yielding the simple formula

$$sI \simeq (r^2 - 1)/3. \tag{49}$$

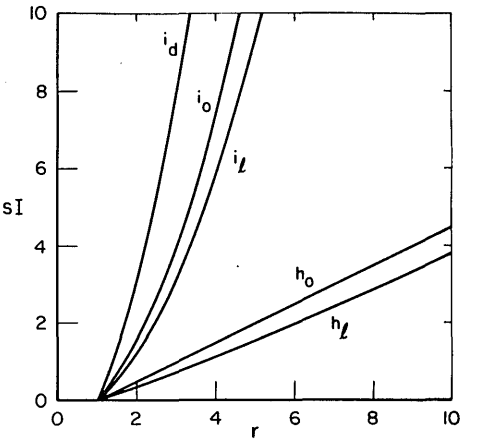

Fig. 4. Normalized internal one-way intensity sI vs the threshold parameter r for various types of lasers. The curve labeled h_o is the homogeneously broadened laser of Eq. (12) neglecting longitudinal spatial hole burning, while h_l denotes the homogeneously broadened laser of Eq. (38) with hole burning included. Similarly, i_o is the inhomogeneously broadened laser of Eq. (14), and i_l is the laser of Eq. (45). The curve i_d is the extreme case of a Doppler laser described by Eq. (50), and most Doppler lasers would be closer to i_o.

C. Doppler Inhomogeneous Broadening

The subject of gain saturation and power in gas lasers is somewhat more complicated than the same topics applied to most common solid or liquid lasers. The basic reason for this added complexity is the inevitable rapid motion of the lasing atoms or molecules. The Doppler shifts resulting from this motion may cause the light waves propagating to the right to interact with a different velocity class of atoms from that seen by the light waves propagating left. Furthermore, during their excited-state lifetimes the atoms may be able to move across the nodes and maxima that constitute the standing wave saturating field. Such motion will be found to reduce the longitudinal spatial hole burning and increase the laser intensity.

The basic equations governing the intensity and frequency in a Doppler broadened laser are given as (A54) and (A55):

$$\frac{1}{r} = \int_{-\infty}^{\infty} \frac{N(v)W_r(v)dv}{1 + 2W_r(v)sI} \Big/ \int_{-\infty}^{\infty} N(v)\alpha_{or}(v)dv, \tag{50}$$

$$\frac{2(\omega - \Omega)t_c}{r} = \int_{-\infty}^{\infty} N(v)\,\mathrm{Re}\left[\frac{\omega_0 - \omega}{ikv + \gamma}\frac{W(v)}{1 + 2W_r(v)sI}\right] dv \Big/ \int_{-\infty}^{\infty} N(v)\alpha_{or}(v)dv, \tag{51}$$

where $N(v)$ is the velocity dependent population inversion. The function $W(v)$ is expressed in Eq. (A50) as a continued fraction involving the optical frequency and intensity of the laser field together with the velocity and lifetimes of the laser atoms or molecules. For the present application the mode pulling implied by Eq. (51) can be neglected. Before considering the general implications of Eq. (50), it can be observed that this equation must include homogeneous broadening as a special case. To obtain this limit one may simply set $N(v)$ equal to a δ function centered at $v = 0$. Thus $\alpha_j(v)$ of Eq. (A46) reduces to a real Lorentzian, and $\beta_j(v)$ of Eq. (A48) reduces to unity. The continued fraction $W(v)$ can be readily summed and one regains Eq. (32), as should be expected for this limit.

The general relationship between r and sI that is implied by Eq. (50) must be evaluated numerically and an example is shown in Fig. 4. For this example it has been assumed that there are no phase interrupting collisions ($\gamma_{ph} = 0$), the other decay rates are equal ($\gamma_a = \gamma_b = \gamma$), and the laser is tuned to line center to maximize spatial hole burning ($\omega = \omega_0$). Furthermore, the laser is strongly inhomogeneously broadened so that the inversion $N(v)$ may be replaced by a constant and cancelled from the right-hand side of Eq. (50). It may be seen from the figure that the present very cumbersome solution differs but slightly from the results obtained for a non-Doppler inhomogeneously broadened laser neglecting spatial hole burning entirely. Thus the motion of the atoms or molecules is highly effective at smoothing out the spatial holes. Apparently, the standing wave nature of the fields causes a slight in-

crease in the laser efficiency as all the lasing atoms are able to interact with the field maxima.

It is important to note that, for many applications, Eq. (50) can be replaced by a much simpler approximate relationship. From Eq. (A48) it follows that the peak value of the function $\beta_1(v)$ at velocity $v = 0$ is always unity. The width of this function, however, is characterized by the smaller of $\gamma_a/2k$ and $\gamma_b/2k$. The function $\alpha_0(v)$, on the other hand, has one or two peaks (depending on the value of $\omega - \omega_0$), which are characterized by the width γ/k. It then follows from the form of $W(v)$ in Eq. (A50) that, in any velocity integration, $\beta_1(v)$ may simply be replaced by zero as long as γ_a or γ_b or both are much smaller than γ. The same result applies if the laser is tuned away from line center such that $\omega - \omega_0$ is greater than the smaller of γ_a and γ_b. But these cases include the vast majority of practical lasers, and it usually happens that γ_a is much smaller than γ_b. The only time that the full continued fraction form of $W(v)$ would be required would be in a laser tuned near line center with $\gamma_a \sim \gamma_b$ and negligible pressure broadening ($\gamma \gg \gamma_{ph}$). Such a system would not often be encountered in practice, and one is usually safe in replacing $W(v)$ with $\alpha_0(v)$. Thus Eq. (50) becomes

$$\frac{1}{r} = \int_{-\infty}^{\infty} \frac{N(v)\alpha_{or}(v)dv}{1 + 2\alpha_{or}(v)sI} \Big/ \int_{-\infty}^{\infty} N(v)\alpha_{or}(v)dv$$

$$= \int_{-\infty}^{\infty} \frac{N(v)dv}{\left[\dfrac{\gamma^2/2}{\gamma^2 + (kv + \omega - \omega_0)^2} + \dfrac{\gamma^2/2}{\gamma^2 + (kv - \omega + \omega_0)^2}\right]^{-1} + 2sI}$$

$$\div \int_{-\infty}^{\infty} \left[\frac{\gamma^2/2}{\gamma^2 + (kv + \omega - \omega_0)^2} + \frac{\gamma^2/2}{\gamma^2 + (kv + \omega - \omega_0)^2}\right] N(v)dv. \tag{52}$$

If the laser is tuned to line center ($\omega = \omega_0$), Eq. (52) reduces to

$$\frac{1}{r} = \int_{-\infty}^{\infty} \frac{N(v)dv}{1 + (kv/\gamma)^2 + 2sI} \Big/ \int_{-\infty}^{\infty} \frac{N(v)dv}{1 + (kv/\gamma)^2}. \tag{53}$$

For strong inhomogeneous broadening the integrals are elementary, and one finds $sI = (r^2 - 1)/2$, the same as Eq. (14). This result accounts for the reasonably close agreement in Fig. 4 between the Doppler case with spatial hole burning and the non-Doppler case without spatial hole burning. The Doppler example in Fig. 4 is actually a worst-case for the approximation given in Eq. (52). Other exact numerical solutions have also been obtained, and it may be noted that, with the single change $\gamma_a = 0.1\ \gamma_b$, the exact solutions are indistinguishable in the figure from the approximate results.

In concluding this section it might be worth mentioning that the longitudinal spatial hole burning effects that have been considered include most of the basic broad categories of lasers. Needless to say, there are additional complicating factors that may be important in certain cases. Among these are drift and diffusion of the lasing atoms and molecules. For a discussion of these complications from a rate equation point of view the reader is referred to Ref. 12. It might also be noted that longitudinal spatial hole burning is usually regarded as an undesirable effect because of its reduction in laser intensity and its encouragement of complex multimode effects. Accordingly, various techniques have been developed to eliminate this effect including operation as a one-directional ring laser,[7] longitudinal translation of the cavity mode with respect to the amplifying medium,[12] or twisting the mode with internal birefringent plates.[13]

V. Transverse Spatial Hole Burning

A. Homogeneous Broadening

When calculating the power characteristics of a laser amplifier or oscillator, one typically assumes that the intensity is roughly uniform over some cross section. Then the usual 1-D saturation results are used. In actual lasers, however, it is always the case that the intensity has a nonuniform spatial dependence. Here the possibility of extending the saturation equations to 3-D situations is investigated. The principal assumption made is that the form of the laser mode is known, and that only the total power is to be determined. The magnitude of the errors involved in the 1-D approximation is determined, and some useful saturation formulas are derived.

In most practical lasers the beams are nearly plane waves. Thus the intensity at any point can be factored into two parts as

$$I(r,\phi,z) = P(z)f(r,\phi,z), \tag{54}$$

where $P(z)$ describes the z dependence of the power, and $f(r,\phi,z)$ is a normalized function describing the variation of the intensity over any cross section of the beam. For this discussion $f(r,\phi,z)$, the mode structure, is presumed known, while $P(z)$ is to be determined. In particular we assume that the field distribution is the normalized Gaussian

$$f(r,\phi,z) = [2/\pi w^2(z)] \exp[-2r^2/w^2(z)], \tag{55}$$

where $w(z)$ is the $1/e$ amplitude spot size.

From Eq. (8) the formula for the line center intensity saturation in a homogeneously broadened laser amplifier is

$$\frac{dI}{dz} = \frac{g_{ho}I}{1 + sI} - \eta I. \tag{56}$$

If Eqs. (54) and (55) are substituted into Eq. (56), the result can be integrated over the beam cross section to obtain a differential equation for the power in the beam

$$\frac{dP}{dz} = \frac{g_{ho}\pi w^2}{2s} \ln\left(1 + \frac{2sP}{\pi w^2}\right) - \eta P. \tag{57}$$

This equation provides a good description of the power in a beam propagating through a laser amplifier, as long as the amplitude distribution remains approximately Gaussian.

A similar equation can also be obtained for describing the power in a low-gain laser oscillator. For this purpose the saturating intensity should be doubled to ac-

count for the right and left traveling beams, and Eq. (18) is replaced by

$$\frac{dP}{dz} = \frac{g_{ho}\pi w^2}{4s} \ln\left(1 + \frac{4sP}{\pi w^2}\right) - \eta P. \tag{58}$$

Setting the round-trip gain equal to the round-trip loss as in Sec. II, one finds that the one-way power in the laser cavity is given implicitly by

$$\frac{\pi w^2}{4sP} \ln\left(1 + \frac{4sP}{\pi w^2}\right) = \frac{1}{r}, \tag{59}$$

where r is the threshold parameter. To be specific, it has been assumed that the spot size is effectively constant over the length of the amplifying medium. For comparison with the original approximate results described in Sec. II, it is convenient to introduce the normalized intensity $sI = sP/\pi w^2$. Thus Eq. (59) is

$$\frac{1}{4sI} \ln(1 + 4sI) = \frac{1}{r}. \tag{60}$$

This result is plotted in Fig. 5 along with Eq. (12). From this figure it is clear that the inclusion of a realistic beam profile leads to the prediction of substantially larger (~100%) power output. This discrepancy is largest for operation far above threshold. At large values of r the wings of the beam profile are able to extract energy efficiently from the amplifying medium, so the effective beam area is much greater than πw^2.

B. Inhomogeneous Broadening

The power characteristics of a Gaussian beam in an inhomogeneously broadened laser can also be calculated. As a starting point we take Eq. (13) for a laser tuned to line center. If this equation is combined with Eqs. (54) and (55) for a Gaussian beam and integrated over the beam profile, one obtains the power equation

$$\frac{dP}{dz} = \frac{g_i \pi w^2}{s}\left[\left(1 + \frac{2sP}{\pi w^2}\right)^{1/2} - 1\right] - \eta P. \tag{61}$$

In a laser oscillator saturation is caused by the sum of the right and left traveling intensities, and Eq. (61) is replaced by

$$\frac{dP}{dz} = \frac{g_i \pi w^2}{2s}\left[\left(1 + \frac{4sP}{\pi w^2}\right)^{1/2} - 1\right] - \eta P. \tag{62}$$

Setting the round-trip gain equal to the round-trip loss leads to the power equation

$$\frac{\pi w^2}{2sP}\left[\left(1 + \frac{4sP}{\pi w^2}\right)^{1/2} - 1\right] = \frac{1}{r}. \tag{63}$$

This equation can also be inverted, and the power is then given explicitly by

$$\frac{sP}{\pi w^2} = r(r - 1). \tag{64}$$

In terms of the normalized intensity $sI = sP/\pi w^2$, this is simply

$$sI = r(r - 1). \tag{65}$$

Equation (65) is plotted in Fig. 5. Also shown is our earlier approximation $sI = (r^2 - 1)/2$, which corresponds to a uniform beam of cross section πw^2. It is clear from this comparison that, as before, the Gaussian beam profile results in a much larger power. For completeness we note that the formulas obtained are strictly applicable only for non-Doppler broadening or for Doppler broadening when the laser frequency is tuned close to line center. For a detuned Doppler laser the right and left traveling intensities interact with different atoms. The result of a power calculation in this case is that the power is simply doubled, and the lines corresponding to i_t and i_o in Fig. 5 should be shifted upward by a factor of 2.

It should also be noted that this same procedure applies equally well for other beam profiles. Thus one might repeat these calculations for Laguerre-Gaussian, Hermite-Gaussian, astigmatic or slab-geometry beams, or the sinusoidal and Bessel function modes occurring in waveguide lasers. While more difficulty might be encountered in the integrations, the results should be qualitatively the same. As with longitudinal spatial hole burning, diffusion may sometimes be important, particularly in lasers with long excited-state lifetimes.[14]

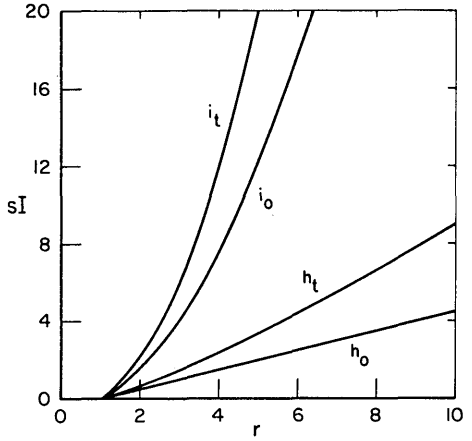

Fig. 5. Normalized intensity sI vs the threshold parameter r for various lasers. The curve labeled h_o is the homogeneously broadened laser of Eq. (12) neglecting transverse spatial hole burning, while h_t denotes the laser of Eq. (60). Similarly, i_o is the inhomogeneously broadened laser of Eq. (14), and i_t is the laser of Eq. (65).

VI. Mixed Broadening

In all the preceding calculations it has been assumed that the laser could be regarded as being either homogeneously or inhomogeneously broadened. In fact, of course, the line broadening of every real laser lies somewhere in between these two idealized limits. For practical applications it is, therefore, essential to understand first the magnitude of any competing broadening processes. Once this has been determined, it still is useful to be able to estimate the errors that might result from assuming that the line broadening is either

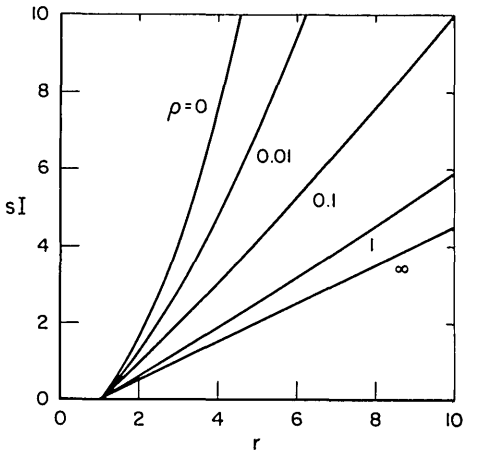

Fig. 6. Normalized intensity sI vs the threshold parameter r for various values of the mized broadening parameter ρ. For small values of ρ the curve approaches the relationship of Eq. (14), and for large ρ the curve approaches Eq. (12).

purely homogeneous or purely inhomogeneous. It is always desirable to be able to assume one of these pure cases because of the resulting simplification in the analysis.

The effects of mixed broadening can be best estimated by solving exactly what is probably the most common example. Thus we consider the case of a gas laser with comparable levels of Doppler and homogeneous broadening. For line center tuning the governing equation is (53), and this can be written explicitly as

$$\frac{1}{r} = \int_{-\infty}^{\infty} \frac{\exp(-v^2/u^2)dv}{1+(kv/\gamma)^2+2sI} \Big/ \int_{-\infty}^{\infty} \frac{\exp(-v^2/u^2)dv}{1+(kv/\gamma)^2}, \quad (66)$$

where u is the average speed of the atoms. It is convenient to introduce the normalized velocity $y = kv/\gamma$ and the broadening parameter $\rho = \gamma^2/(k^2u^2)$. Then Eq. (66) takes the form

$$\frac{1}{r} = \int_{-\infty}^{\infty} \frac{\exp(-\rho y^2)dy}{1+y^2+2sI} \Big/ \int_{-\infty}^{\infty} \frac{\exp(-\rho y^2)dy}{1+y^2}. \quad (67)$$

In the notation of Sec. II these new parameters would have the values $y = 2(\nu_0 - \nu_a)/\Delta\nu_h$ and $\rho = \Delta\nu_h^2 \ln 2/\Delta\nu_D^2$.

Equation (67) is plotted in Fig. 6 for various values of ρ. Not surprisingly, for small values of ρ the curve approaches the inhomogeneous limit $sI = (r^2 - 1)/2$, and for large values of ρ the curve approaches the homogeneous limit $sI = (r - 1)/2$. The most significant aspect of these curves is that the case of truest mixed broadening occurs with $\rho \simeq 0.1$ rather than occurring with $\rho \simeq 1$, as one might have expected. Thus, when it is mathematically important to identify a laser as either homogenenous or inhomogeneous, the transition between these types should be considered to occur at about $\rho = 0.1$.

Another interesting feature of Fig. 6 is the general similarity of the curves for all values of ρ, and one is led to inquire whether Eq. (67) might be reasonably approximated by a relationship of the form

$$sI = [r^{f(\rho)} - 1]/2. \quad (68)$$

It would be especially useful if such a relationship could be found for the most common operating regime near threshold ($r \lesssim 2$). For this purpose Eq. (67) may be expanded for small values of sI, and one readily finds

$$f(\rho) = \int_0^{\infty} \frac{\exp(-\rho y^2)dy}{1+y^2} \Big/ \int_0^{\infty} \frac{\exp(-\rho y^2)dy}{(1+y^2)^2}. \quad (69)$$

The numerator of this ratio is the error function,[15] and, with the change of variables $x = y^2$, the denominator is recognizable as a Whittaker function.[16]

Equation (69) is plotted in Fig. 7. As expected, for small values of ρ the limit is one. Using Fig. 7 and Eq. (68) one can readily determine the intensity in a laser with arbitrary mixed broadening. If these results are compared to the exact solutions of Fig. 6, one finds that the approximation holds well for r as large as two or three.

In some cases it is helpful to have a fully analytic expression for the intensity, and the simple form of the curve in Fig. 7 suggests some analytic approximations. For example, there is some resemblance to the Fermi distribution, and one readily finds the best fit is

$$f(\rho) \simeq 1 + \frac{1}{1+\exp[\zeta(\log\rho - \log\rho_0)]}, \quad (70)$$

with $\rho_0 = 0.12$, and $\zeta = 1.4$.

VII. Conclusion

Any calculation of the power characteristics of a laser oscillator involves several approximations. In this paper we have examined some of the most fundamental of these approximations to see how large the corresponding errors might be. For uniformity the results have been summarized in a set of plots of intensity vs the threshold parameter. In brief one can observe from

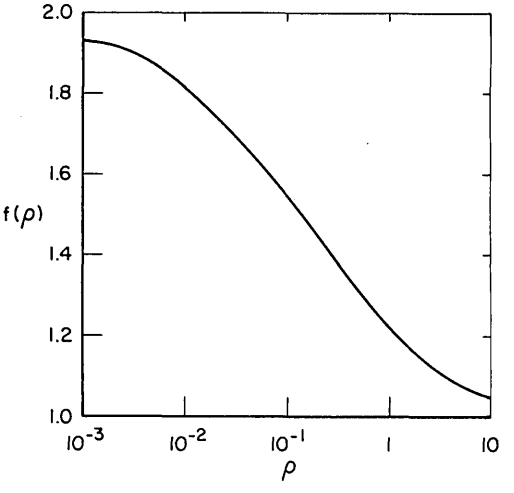

Fig. 7. Saturation exponent as a function of the mixed broadening parameter ρ.

these plots that, in lasers having a large single-pass gain, the intensity can be an order of magnitude higher than expected from the low-gain formulas. Longitudinal spatial hole burning typically causes an intensity reduction of 20–30% in comparison to the standard formulas for homogeneously broadened or inhomogeneously broadened lasers. Transverse spatial hole burning may cause an increase in intensity by about 100%. Very large errors also may result if one does not correctly identify the dominant type of line broadening, and simple formulas have been given for estimating the power characteristics of lasers with mixed broadening. Although it is not feasible to account simultaneously for all these error types, one may reasonably expect that, when each type is small, the effect will be cumulative. Extensive experimental confirmation of the high-gain formulas exists in the literature, and it is likely that more careful studies of the other effects discussed here will be possible in light of the new formulas. It is also anticipated that the use of such formulas, which are often almost as simple as the approximations, might lead to substantial savings in time and cost in the laser design process. Greater accuracy should also be possible in the familiar problem of inferring the characteristics of a laser component from the behavior of a laser oscillator system.

The author is pleased to acknowledge valuable discussions with Kendall C. Reyzer.

Appendix: Longitudinal Spatial Hole Burning

1. Saturation Equations

Before a rigorous discussion of longitudinal spatial hole burning can be undertaken, it is necessary to set down the equations that govern the interaction of light with atoms on a small scale. The most generally useful starting point is a semiclassical approach using Maxwell's equations coupled to the density matrix equations. The equations governing the ensemble averaged density matrix can be written[17]

$$\left(\frac{\partial}{\partial t}+v\frac{\partial}{\partial z}\right)\rho_{ab}(v,\omega_a,z,t)=-(i\omega_a+\gamma)\rho_{ab}(v,\omega_a,z,t)-\frac{i\mu}{\hbar}E(z,t)[\rho_{aa}(v,\omega_a,z,t)-\rho_{bb}(v,\omega_a,z,t)], \quad (A1)$$

$$\left(\frac{\partial}{\partial t}+v\frac{\partial}{\partial z}\right)\rho_{aa}(v,\omega_a,z,t)=\lambda_a(v,\omega_a,z,t)-\gamma_a\rho_{aa}(v,\omega_a,z,t)+\left[\frac{i\mu}{\hbar}E(z,t)\rho_{ba}(v,\omega_a,z,t)+\text{c.c.}\right], \quad (A2)$$

$$\left(\frac{\partial}{\partial t}+v\frac{\partial}{\partial z}\right)\rho_{bb}(v,\omega_a,z,t)=\lambda_b(v,\omega_a,z,t)-\gamma_b\rho_{bb}(v,\omega_a,z,t)-\left[\frac{i\mu}{\hbar}E(z,t)\rho_{ba}(v,\omega_a,z,t)+\text{c.c.}\right], \quad (A3)$$

$$\rho_{ba}(v,\omega_a,z,t)=\rho^*_{ab}(v,\omega_a,z,t), \quad (A4)$$

where γ_a and γ_b represent the decay rates of the diagonal matrix elements, $\gamma=(\gamma_a+\gamma_b)/2+\gamma_{ph}$ is the decay for the off-diagonal elements, λ_a and λ_b are the pumping terms, and ω_a is the center frequency of the laser transition for members of atomic class a. Maxwell's wave equation for the electric field of a linearly polarized wave in a laser medium can be written

$$\frac{\partial^2E(z,t)}{\partial z^2}-\mu_0\sigma\frac{\partial E(z,t)}{\partial t}-\mu_0\epsilon_0\frac{\partial^2E(z,t)}{\partial t^2}=\mu_0\frac{\partial^2P(z,t)}{\partial t^2}. \quad (A5)$$

The polarization driving this wave equation can be related back to the off-diagonal matrix elements by

$$P(z,t)=\int_0^\infty\int_{-\infty}^\infty\mu\rho_{ab}(v,\omega_a,z,t)dvd\omega_a+\text{c.c.}, \quad (A6)$$

where μ is the dipole moment.

In cw oscillation the rapid time and space dependence of the electric field and off-diagonal matrix elements can be factored out by means of the substitutions

$$E(z,t)=\tfrac{1}{2}E'\sin(kz)\exp(-i\omega t)+\text{c.c.}, \quad (A7)$$

$$\rho_{ab}(v,\omega_a,z,t)=[C(v,\omega_a,z)+iS(v,\omega_a,z)]\exp(-i\omega t)/2\mu. \quad (A8)$$

With the standard rotating-wave approximation, Eqs. (A1)–(A4) reduce to

$$v\frac{\partial}{\partial z}S(v,\omega_a,z)=(\omega-\omega_a)C(v,\omega_a,z)-\gamma S(v,\omega_a,z)-\frac{\mu^2}{\hbar}E'D(v,\omega_a,z)\sin(kz), \quad (A9)$$

$$v\frac{\partial}{\partial z}C(v,\omega_a,z)=-(\omega-\omega_a)S(v,\omega_a,z)-\gamma C(v,\omega_a,z), \quad (A10)$$

$$v\frac{\partial}{\partial z}D(v,\omega_a,z)=\lambda_a(v,\omega_a)-\lambda_b(v,\omega_a)-\frac{\gamma_a+\gamma_b}{2}D(v,\omega_a,z)-\frac{\gamma_a-\gamma_b}{2}M(v,\omega_a,z)+\frac{E'}{\hbar}S(v,\omega_a,z)\sin(kz), \quad (A11)$$

$$v\frac{\partial}{\partial z}M(v,\omega_a,z)=\lambda_a(v,\omega_a)+\lambda_b(v,\omega_a)-\frac{\gamma_a+\gamma_b}{2}M(v,\omega_a,z)-\frac{\gamma_a-\gamma_b}{2}D(v,\omega_a,z), \quad (A12)$$

where $D=\rho_{aa}-\rho_{bb}$ is the population difference, and $M=\rho_{aa}+\rho_{bb}$ is the population sum. Similarly, wave

Eq. (A5) reduces to the set

$$\frac{\sigma}{2\epsilon_0}E' = -\frac{\omega_0}{\epsilon_0 L}\int_{-\infty}^{\infty}\int_0^{\infty}\int_0^{l}\sin(kz)S(v,\omega_a,z)dzd\omega_a dv, \quad \text{(A13)}$$

$$(\omega-\Omega)E' = -\frac{\omega_0}{\epsilon_0 L}\int_{-\infty}^{\infty}\int_0^{\infty}\int_0^{l}\sin(kz)C(v,\omega_a,z)dzd\omega_a dv, \quad \text{(A14)}$$

where the rotating-wave approximation has been employed, real and imaginary parts have been isolated, and both sides have been multiplied by $\sin(kz)$ and integrated over z.

Equations (A9)–(A14) represent six equations in the unknowns S, C, D, M, E', and ω. They may be solved numerically, but for most practical applications further analytical reductions are possible. To proceed with these calculations it is necessary to specify the dominant line broadening mechanisms.

2. Non-Doppler Broadening

In many practical laser media the broadening due to Doppler shifts is small compared with broadening by unequal atomic center frequencies or homogeneous processes such as natural and collisional broadening. Doppler effects can be eliminated by setting v equal to zero on the left-hand sides of Eqs. (A9)–(A12) and integrating over velocity. The results of these operations are

$$0 = (\omega-\omega_a)C(\omega_a,z) - \gamma S(\omega_a,z) - \frac{\mu^2}{\hbar}E'D(\omega_a,z)\sin(kz), \quad \text{(A15)}$$

$$0 = -(\omega-\omega_a)S(\omega_a,z) - \gamma C(\omega_a,z), \quad \text{(A16)}$$

$$0 = \lambda_a(\omega_a) - \lambda_b(\omega_a) - \frac{\gamma_a+\gamma_b}{2}D(\omega_a,z) - \frac{\gamma_a-\gamma_b}{2}M(\omega_a,z) + \frac{E'}{\hbar}S(\omega_a,z)\sin(kz), \quad \text{(A17)}$$

$$0 = \lambda_a(\omega_a) + \lambda_b(\omega_a) - \frac{\gamma_a+\gamma_b}{2}M(\omega_a,z) - \frac{\gamma_a-\gamma_b}{2}D(\omega_a,z), \quad \text{(A18)}$$

$$\frac{\sigma}{2\epsilon_0}E' = -\frac{\omega_0}{\epsilon_0 L}\int_0^{\infty}\int_0^{l}\sin(kz)S(\omega_a,z)dzd\omega_a, \quad \text{(A19)}$$

$$(\omega-\Omega)E' = -\frac{\omega_0}{\epsilon_0 L}\int_0^{\infty}\int_0^{l}\sin(kz)C(\omega_a,z)dzd\omega_a, \quad \text{(A20)}$$

where we have introduced the new definitions

$$S(\omega_a,z) = \int_{-\infty}^{\infty}S(v,\omega_a,z)dv,\ C(\omega_a,z) = \int_{-\infty}^{\infty}C(v,\omega_a,z)dv,$$

$$D(\omega_a,z) = \int_{-\infty}^{\infty}D(v,\omega_a,z)dv,\ M(\omega_a,z) = \int_{-\infty}^{\infty}M(v,\omega_a,z)dv,$$

$$\lambda_a(\omega_a) = \int_{-\infty}^{\infty}\lambda_a(v,\omega_a)dv,\ \lambda_b(\omega_a) = \int_{-\infty}^{\infty}\lambda_b(v,\omega_a)dv.$$

The in-phase polarization component $C(\omega_a,z)$ can be eliminated from Eqs. (A15) and (A16) yielding

$$S(\omega_a,z) = -\frac{\mu^2E'D(\omega_a,z)\sin(kz)/\gamma\hbar}{1+[(\omega-\omega_a)/\gamma]^2}. \quad \text{(A21)}$$

Similarly, $M(\omega_a,z)$ can be eliminated from Eqs. (A17) and (A18) leaving

$$D(\omega_a,z) = \frac{\gamma_a+\gamma_b}{2\hbar\gamma_a\gamma_b}E'S(\omega_a,z)\sin(kz) + N(\omega_a), \quad \text{(A22)}$$

where the population difference has been defined by

$$N(\omega_a) = \lambda_a(\omega_a)/\gamma_a - \lambda_b(\omega_a)/\gamma_b. \quad \text{(A23)}$$

Combining these equations, the out-of-phase polarization component $S(\omega_a,z)$ can be related directly to the unsaturated population inversion and the intensity according to

$$S(\omega_a,z) = -\frac{\mu^2E'N(\omega_a)\sin(kz)/\gamma\hbar}{1+[(\omega-\omega_a)/\gamma]^2+4\sin^2(kz)sI}, \quad \text{(A24)}$$

where the normalized intensity is defined by

$$sI = \frac{\mu^2E'^2}{8\hbar^2}\frac{\gamma_a+\gamma_b}{\gamma\gamma_a\gamma_b}. \quad \text{(A25)}$$

With Eq. (A16), the polarization component $C(\omega_a,z)$ is

$$C(\omega_a,z) = \left(\frac{\omega-\omega_a}{\gamma}\right)\frac{\mu^2E'N(\omega_a)\sin(kz)/\gamma\hbar}{1+[(\omega-\omega_a)/\gamma]^2+4\sin^2(kz)sI}. \quad \text{(A26)}$$

Equations (A19), (A20), (A24), and (A26) may be combined yielding

$$\frac{1}{2t_c} = \frac{\omega_0\mu^2}{\epsilon_0 L\gamma\hbar}\int_0^{\infty}\int_0^{l}\frac{\sin^2(kz)N(\omega_a)dzd\omega_a}{1+[(\omega-\omega_a)/\gamma]^2+4\sin^2(kz)sI}, \quad \text{(A27)}$$

$$\omega-\Omega = \frac{\omega_0\mu^2}{\epsilon_0 L\gamma\hbar}\int_0^{\infty}\int_0^{l}\left(\frac{\omega_a-\omega}{\gamma}\right)\times\frac{\sin^2(kz)N(\omega_a)dzd\omega_a}{1+[(\omega-\omega_a)/\gamma]^2+4\sin^2(kz)sI}. \quad \text{(A28)}$$

This is a coupled set of equations governing the intensity and frequency of the oscillating mode in a non-Doppler broadened laser. These results appear as Eqs. (28) and (29) in the text.

3. Doppler Broadening

In the limit that Doppler broadening dominates other broadening processes, Eqs. (A9)–(A14) reduce to

$$v\frac{\partial}{\partial z}S(v,z) = (\omega-\omega_0)C(v,z) - \gamma S(v,z) - \frac{\mu^2}{\hbar}E'D(v,z)\sin(kz), \tag{A29}$$

$$v\frac{\partial}{\partial z}C(v,z) = -(\omega-\omega_0)S(v,z) - \gamma C(v,z), \tag{A30}$$

$$v\frac{\partial}{\partial z}D(v,z) = \lambda_a(v) - \lambda_b(v) - \frac{\gamma_a+\gamma_b}{2}D(v,z) - \frac{\gamma_a-\gamma_b}{2}M(v,z) + \frac{E'}{\hbar}S(v,z)\sin(kz), \tag{A31}$$

$$v\frac{\partial}{\partial z}M(v,z) = \lambda_a(v) + \lambda_b(v) - \frac{\gamma_a+\gamma_b}{2}M(v,z) - \frac{\gamma_a-\gamma_b}{2}D(v,z), \tag{A32}$$

$$\frac{\sigma}{2\epsilon_0}E' = -\frac{\omega_0}{\epsilon_0 L}\int_{-\infty}^{\infty}\int_0^l \sin(kz)S(v,z)dzdv, \tag{A33}$$

$$(\omega-\Omega)E' = -\frac{\omega_0}{\epsilon_0 L}\int_{-\infty}^{\infty}\int_0^l \sin(kz)C(v,z)dzdv, \tag{A34}$$

where Eqs. (A9)–(A12) have been integrated over ω_a using the definitions

$$S(v,z) = \int_{-\infty}^{\infty} S(v,\omega_a,z)d\omega_a, \quad C(v,z) = \int_{-\infty}^{\infty} C(v,\omega_a,z)d\omega_a,$$

$$D(v,z) = \int_{-\infty}^{\infty} D(v,\omega_a,z)d\omega_a, \quad M(v,z) = \int_{-\infty}^{\infty} M(v,\omega_a,z)d\omega_a.$$

Now it is helpful to eliminate the z derivatives by expanding the polarization and population elements in series of spatial harmonics according to

$$S(v,z) = \sum_{j=-\infty}^{\infty} S_{2j+1}(v)\exp[(2j+1)ikz], \tag{A35}$$

$$C(v,z) = \sum_{j=-\infty}^{\infty} C_{2j+1}(v)\exp[(2j+1)ikz], \tag{A36}$$

$$D(v,z) = \sum_{j=-\infty}^{\infty} D_{2j}(v)\exp[(2j)ikz], \tag{A37}$$

$$M(v,z) = \sum_{j=-\infty}^{\infty} M_{2j}(v)\exp[(2j)ikz], \tag{A38}$$

subject to the constraints $S_\alpha(v) = S^*_{-\alpha}(v)$, $C_\alpha(v) = C^*_{-\alpha}(v)$, etc. These constraints ensure that Eqs. (A29)–(A34) remain real, and one now obtains the spatially independent set

$$0 = -[(2j+1)ikv+\gamma]S_{2j+1}(v) + (\omega-\omega_0)C_{2j+1}(v) + \frac{i\mu^2E'}{2\hbar}[D_{2j}(v) - D_{2j+2}(v)], \tag{A39}$$

$$0 = -[(2j+1)ikv+\gamma]C_{2j+1}(v) - (\omega-\omega_0)S_{2j+1}(v), \tag{A40}$$

$$0 = [\lambda_a(v) - \lambda_b(v)]\delta_{jo} - \left[(2j)ikv + \frac{\gamma_a+\gamma_b}{2}\right]D_{2j}(v) - \frac{\gamma_a-\gamma_b}{2}M_{2j}(v) - \frac{iE'}{2\hbar}[S_{2j-1}(v) - S_{2j+1}(v)], \tag{A41}$$

$$0 = [\lambda_a(v) + \lambda_b(v)]\delta_{jo} - \left[(2j)ikv + \frac{\gamma_a+\gamma_b}{2}\right]M_{2j}(v) - \frac{\gamma_a-\gamma_b}{2}D_{2j}(v), \tag{A42}$$

$$\frac{E'}{2t_c} = \frac{\omega_0 l}{\epsilon_0 L}\int_{-\infty}^{\infty} S_{1i}(v)dv, \tag{A43}$$

$$(\omega-\Omega)E' = \frac{\omega_0 l}{\epsilon_0 L}\int_{-\infty}^{\infty} C_{1i}(v)dv, \tag{A44}$$

where the subscript i refers to the imaginary part.

Equations (A39)–(A44) may be combined to obtain two coupled equations for the oscillation amplitude E' and frequency ω.[16] First Eqs. (A39) and (A40) are combined yielding

$$S_{2j+1}(v) = \frac{i\mu^2E'}{2\hbar\gamma}\alpha_j(v)[D_{2j}(v) - D_{2j+2}(v)], \tag{A45}$$

where $\alpha_j(v)$ is defined by

$$\alpha_j(v) = \frac{\gamma/2}{(2j+1)ikv + i(\omega-\omega_0) + \gamma} + \frac{\gamma/2}{(2j+1)ikv - i(\omega-\omega_0) + \gamma}. \tag{A46}$$

Similarly, Eqs. (A41) and (A42) may be combined yielding

$$D_{2j}(v) = -\frac{iE'}{4\hbar}\frac{\gamma_a+\gamma_b}{\gamma_a\gamma_b}\beta_j(v)[S_{2j-1}(v) - S_{2j+1}(v)] + \left[\frac{\lambda_a(v)}{\gamma_a} - \frac{\lambda_b(v)}{\gamma_b}\right]\delta_{jo}, \tag{A47}$$

where $\beta_j(v)$ is defined by

$$\beta_j(v) = \frac{\gamma_a\gamma_b}{\gamma_a+\gamma_b}\left[\frac{1}{(2j)ikv+\gamma_a} + \frac{1}{(2j)ikv+\gamma_b}\right]. \tag{A48}$$

Now Eqs. (A45) and (A47) produce

$$S_1(v) = \frac{i4\hbar}{E'}\frac{\gamma_a\gamma_b}{\gamma_a+\gamma_b}D_0(v)W(v)sI, \tag{A49}$$

where $W(v)$ is the continued fraction

$$W(v) = \cfrac{\alpha_0(v)}{1 + \cfrac{\alpha_0(v)\beta_1(v)sI}{1 + \cfrac{\alpha_1(v)\beta_1(v)sI}{1 + \cfrac{\alpha_1(v)\beta_2(v)sI}{1+\ldots}}}}. \tag{A50}$$

In this result sI is a normalized intensity given by Eq. (A25). With Eq. (A47) for $D_0(v)$ and the condition $S_1(v) = S^*_{-1}(v)$, the imaginary part of $S_1(v)$ is

$$S_{1i}(v) = \frac{4\hbar}{E'}\frac{\gamma_a\gamma_b}{\gamma_a+\gamma_b}\frac{N(v)sIW_r(v)}{1+2W_r(v)sI}, \tag{A51}$$

where $N(v)$ is the unsaturated population difference defined in Eq. (A23), and the subscripts i and r denote, respectively, the imaginary and real parts of a quantity. With Eq. (A40) it follows that the imaginary part of $C_1(v)$ is

$$C_{1i}(v) = \frac{4\hbar}{E'}\frac{\gamma_a\gamma_b}{\gamma_a+\gamma_b}N(v)sI\,\mathrm{Re}\left[\frac{\omega_0-\omega}{ikv+\gamma}\frac{W(v)}{1+2W_r(v)sI}\right]. \tag{A52}$$

Equations (A43) and (A51) may be combined to yield the unsaturated intensity gain coefficient

$$g = \frac{2\omega_0}{c\epsilon_0 E'}\int_{-\infty}^{\infty} S_{1i}(v)dv = \frac{\mu^2\omega_0}{c\epsilon_0\gamma\hbar}\int_{-\infty}^{\infty} N(v)\alpha_{or}(v)dv. \tag{A53}$$

In terms of this gain coefficient Eq. (A43) can be written

$$\frac{1}{t_c} = \frac{gcl}{L} \int_{-\infty}^{\infty} \frac{N(v) W_r(v) dv}{1 + 2W_r(v) sI} \Big/ \int_{-\infty}^{\infty} N(v) \alpha_{or}(v) dv. \quad \text{(A54)}$$

Similarly, Eqs. (A44), (A52), and (A53) may be combined to obtain

$$\omega - \Omega = \frac{gcl}{2L} \int_{-\infty}^{\infty} N(v) \, \mathrm{Re} \left[\frac{\omega_0 - \omega}{ikv + \gamma} \frac{W(v)}{1 + 2W_r(v) sI} \right] dv \Big/ \int_{-\infty}^{\infty} N(v) \alpha_{or}(v) dv. \quad \text{(A55)}$$

Equations (A54) and (A55) are a coupled set that may be solved to obtain the frequency ω and the intensity sI of the cw oscillating mode. In terms of the threshold parameter r they appear in the text as Eqs. (50) and (51).

References

1. A. E. Siegman, *An Introduction to Lasers and Masers* (McGraw-Hill, New York, 1971), Chap. 3.
2. A. Yariv, *Introduction to Optical Electronics* (Holt, Rinehart, and Winston, New York, 1976), Chap. 5.
3. W. E. Lamb, Jr., Phys. Rev. A: **134,** 1429 (1964).
4. W. W. Rigrod, J. Appl. Phys. **36,** 2487 (1965).
5. L. W. Casperson, IEEE J. Quantum Electron. **QE-9,** 250 (1973).
6. A similar integration was performed by W. W. Rigrod, J. Appl. Phys. **34,** 2602 (1963).
7. An early discussion of longitudinal spatial hole burning is by C. L. Tang, H. Statz, and G. DeMars, J. Appl. Phys. **34,** 2289 (1963).
8. I. S. Gradshteyn and I. W. Ryzhik, *Table of Integrals, Series, and Products* (Academic, New York, 1965), Eq. (3.615-1).
9. Ref. 8, Eq. (3.681-1).
10. M. Abramowitz and I. A. Stegun, Eds., *Handbook of Mathematical Functions* (U.S. GPO, Washington, D.C., 1970), Eq. (6.2.2).
11. Ref. 10, Eq. (15.1.1).
12. H. G. Danielmeyer, J. Appl. Phys. **42,** 3125 (1971).
13. V. Evtuhov and A. E. Siegman, Appl. Opt. **4,** 142 (1965).
14. O. Ersoy, Opt. Quantum Electron. **7,** 247 (1975).
15. Ref. 8, Eq. (3.466-1).
16. Ref. 8, Eq. (3.383-8).
17. B. J. Feldman and M. S. Feld, Phys. Rev. A: **1,** 1375 (1970).

Meetings Calendar *continued from page 408*

24–28 Laser Safety Course, Washington, D.C. *Laser Inst. Am., P.O. Box 9000, Waco, Tex. 76710*

24–28 Plume Technology Course, U. Tenn. *J. W. Bernard, U. Tenn. Space Inst., Tullahoma, Tenn. 37388*

31–1 Apr. Aging and Human Visual Function Symp., Washington, D.C. *K. Dismukes, NRC Comm. on Vision, 2101 Constitution Ave. N.W., Washington, D.C. 20418*

31–4 Apr. Carbon Dioxine Lasers Course, Denver *Laser Inst. Am., P.O. Box 9000, Waco, Tex. 76710*

April

7–9 Int. Optical Computing Conf., Washington, D.C. *S. Harvitz, Naval Underwater Systems Ctr., New London, Conn. 06320*

7–11 Eleven In-Depth Optical Seminars and Instrument Display, Hyatt Regency Hotel, Washington, D.C. *SPIE, P.O. Box 10, Bellingham, Wash. 98225*

14–18 Laser Applications in Materials Processing Course, Boston *Laser Inst. Am., P.O. Box 9000, Waco, Tex. 76710*

20–22 Applications of Optical Instrumentation in Medicine VII Seminar, MGM Grand Hotel, Las Vegas *SPIE, P.O. Box 10, Bellingham, Wash. 98225*

21–24 APS Mtg., Washington, D.C. *W. W. Havens, Jr., 335 E. 45 St., New York, N.Y. 10017*

21–24 18th INTERMAG Conf., Boston *L. J. Varnerin, Jr., Bell Labs., Murray Hill, N.J. 07974*

21–25 Int. Conf. on Metallurgical Coatings, Holiday Inn at Embarcadero, San Diego *R. F. Bunshah, 6532 Boelter Hall, U. Calif., Los Angeles, Calif. 90024*

22–23 Smoke/Obscurants Symp. IV, Harry Diamond Labs., Adelphi *DRCPM-SMK-T/Mr. Klimek, Aberdeen Proving Ground, Md. 21005*

23–30 Remote Sensing of Environment, 14th Int. Symp., San Jose, Costa Rica *J. J. Cook, ERIM, P.O. Box 8618, Ann Arbor, Mich. 48107*

28–30 Physics of Fiber Optics Conf., Conrad Hilton Hotel, Chicago *S. S. Mitra, Dept. of Elec. Eng., U. R.I., Kingston, R.I. 02881*

30–3 May **Recent Advances in Vision, OSA Topical Mtg.,** Sheraton Sandcastle, Lido Beach, Sarasota, Fla. *OSA, 1816 Jefferson Place N.W., Washington, D. C. 20036*

May

3 **OSA Florida Sec.** Ann. Mtg., U. Central Fla., Orlando *D. Baldwin, 439 Oakhaven Dr., Altamonte Springs, Fla. 32701*

4–8 SPSE 33rd Ann. Conf., Downtown Holiday Inn, Minneapolis *SPSE, 1411 K St. N.W., Suite 930, Washington, D.C. 20005*

5–7 **Basic Optical Properties of Materials, NBS, OSA Topical Conf.,** Gaithersburg *K. Stang, Mater. Bldg. B-348, NBS, Washington, D.C. 20234*